

## Research Article

# Numerical Analysis on the Load Sharing Performance of Long-Short CFG Pile Composite Foundation Subjected to Rotation of Adjacent Retaining Wall

Bantayehu Uba Uge ,<sup>1,2</sup> Yuancheng Guo ,<sup>1</sup> and Yunlong Liu ,<sup>1</sup>

<sup>1</sup>School of Civil Engineering, Zhengzhou University, Zhengzhou 450001, China

<sup>2</sup>School of Civil Engineering, Hawassa University, Hawassa, Ethiopia

Correspondence should be addressed to Yuancheng Guo; [guoyuancheng@163.com](mailto:guoyuancheng@163.com)

Received 9 April 2021; Revised 28 June 2021; Accepted 11 July 2021; Published 22 July 2021

Academic Editor: Zhanbo Cheng

Copyright © 2021 Bantayehu Uba Uge et al. This is an open access article distributed under the Creative Commons Attribution License, which permits unrestricted use, distribution, and reproduction in any medium, provided the original work is properly cited.

The stress and displacement boundary conditions of excavation retaining structures affect the deformation mechanism and movement of the retained soil mass. The soil movement disturbs the load sharing performance and structural integrity of cement-fly ash-gravel (CFG) pile composite foundations existing in the vicinity, which merits considerable research work. This article presents results from 3D finite element analyses performed to study the influence of retaining wall rotation on the load sharing characteristics of adjacent CFG pile composite foundation comprising long and short piles. To verify the numerical model, a relatively large-scale 1 g physical model test was conducted. It is revealed that to arrive at a new static equilibrium during progression of wall rotation, the percentage load sharing ratios of the long and short piles change increasingly while the load proportion carried by the upper soil reduces remarkably. The percentage load sharing characteristics of CFG pile composite foundation are more affected in immediate proximity to the wall than those located at far distance. For the foundation having  $3 \times 3$  long and short piles placed at 3.0–15.0 m away from the wall, the location resulted in a reduction of soil bearing capacity ranging between 1.4 and 7.5% of the total imposed load while the corresponding increase in the % load borne by the long and short pile range was 0.83–4.15 and 0.59–3.36%, respectively. For the other parameters considered in this article viz. pile spacing, subsoil stiffness, cushion stiffness and thickness, and applied working load, the increment in % load sharing of the long and short pile range was 3.45–4.15, 1.3–5.79, 1.48–3.36, 4.15–4.79, and 3.67–4.15% and 3.36–4.67, 1.43–4.99, 1.48–3.36, 3.36–3.64, and 1.38–3.36% of the imposed load, respectively. Moreover, the long piles' load sharing proportion was higher than that of short piles, and peripheral piles received larger load proportion.

## 1. Introduction

Escalating urban land demands and growing population size in emerging cities have promoted the quest for possible alternative solutions to prevailing geotechnical problems, notable among which is enhancing poor ground conditions to make them suitable for construction. Engineers have to choose between the best available foundation treatment method and/or in combination with special foundation system that will allow overlaying structures to satisfy admissible technical requirements. CFG (cement-fly ash-gravel) pile composite foundation with mechanical

characteristics intermediate between conventional shallow and deep foundations is generally a disconnected type of piled raft foundation that serves to achieve the performance requirements in almost all kinds of weak soils to support high-rise buildings and other infrastructures [1]. The concept is more popular across Europe and Asia where serviceability requirement for mat foundation calls for the use of settlement reducing piles [2]. The CFG piles crowned with a cushion layer receive the foundation load indirectly; and owing to the deformability characteristics of the cushion, piles' head pricks into the mattress layer, leading to relative pile/soil settlement that provokes negative side friction

(NSF) to develop on the upper 15–50% of the pile length [3–7]. In this regard, researchers such as Halder and Manna [3], Rui et al. [4], and Fioravante and Giretti [8] conducted centrifuge and static geotechnical model tests, and Tradigo et al. [6] and Ata et al. [9] performed numerical analyses while Jiang and Liu [5] and Wu et al. [7] established differential equation based on typical unit calculation model to deduce the calculation formula of the depth of neutral plane and pile-soil stress ratio.

In order to meet further economic advantages of CFG pile reinforced ground, a combination of different piles with varying stiffness [10, 11] and/or length [12, 13] has been used in practice. Earlier studies have disclosed that the natural unfavourable shallow soil would be strengthened by the short/flexible piles whereas the long piles play a major role in reducing the foundation settlement. Moreover, the influence of various components such as cushion's property and geometry, subgrade material stiffness properties, geometric and stiffness properties of piles, and raft thickness on the vertical load sharing proportion between the piles and soil and overall foundation settlement characteristics have been discussed by a number of authors [14–16]. The recent experimental study of Guo et al. [17] on the pile-soil synergistic mechanism of such multipile foundation system revealed a significant influence of long piles relative to the short ones on overall settlement and stiffness of the foundation under vertical working load. In reality, however, a foundation system is not only subject to vertical loading but also to lateral loadings [18–20]. Ma et al. [18] conducted experimental and numerical study using ANSYS software to investigate the bearing characteristics of long-short pile composite foundation subjected to horizontal forces while Zhu et al. [20] studied the horizontal bearing characteristics of disconnected piled rafts with equal length piles subjected to lateral loads. It can be seen from the results of these studies that under both vertical and lateral loads, the interposed layer plays a significant role as it adjusts the vertical load sharing while offering horizontal resistance to the lateral load by the friction developing at its interface with the other contacting materials. Nonetheless, studies on horizontal load bearing behaviour are still limited, probably because of the complex soil structure interaction.

In recent years, the safety of conventional pile foundation subjected to ground movements arising from nearby excavations and/or other sources has particularly garnered the attention of scholars globally [21–24]. This is because the risk associated with foundation pit excavation-induced phenomenon could bring about causalities and huge economic losses as a result of catastrophic collapse of infrastructures [25–27]. To avoid such undesirable events, stringent performance requirements are nowadays put as risk control measures for the safety of neighbouring facilities in congested municipalities. Along with this, scholars [28, 29] have suggested that lessons taken from previous foundation pit excavation failures could potentially be beneficial in preventing future failure events. According to Poulos [19], the mechanism of loading arising from ground movements is different in action to that of lateral loadings

acting on the pile head and even if the ultimate bearing capacity may not be affected, the load from such hidden sources has a significant influence on adjacent piles. In the same manner, the lateral ground disturbances associated with the process of excavation affect the load sharing mechanism of nearby CFG pile composite foundations [30].

The schematic representation in Figure 1 illustrates a typical noncontact long-short piled raft foundation situated at a distance  $x_0$  away from an excavation of depth  $H_e$  retained by a retaining wall embedded to a depth  $H_p$  below the dredge line. The common pile to pile spacing in composite foundation usually ranges from 2 to 5 times the pile diameter; and the outward projection of the mat edge from the outer pile is 1.5 to 2 times the pile diameter [31]. Unless the excavation-induced deformation of the support structure is kept under control within a very small range, the resulting soil movement would influence the performance of such foundations in immediate vicinity, especially if they exist within excavation influence zone. Nevertheless, in recent years, many efforts have been made toward development and distribution of lateral earth pressure acting on retaining wall neighbouring composite foundations [32, 33]. This is because of the lateral reinforcement effect of CFG piles that cannot be ignored and has to be acknowledged to optimize the rigidity and working mechanism of foundation pit support structures [34]. For instance, when it comes to the active earth pressure acting on the wall, studies have shown that the calculation results obtained from the conventional theories are normally larger than experimental observations [33, 35] and numerical findings [36] due the shielding effect of the CFG piles. According to Wei [37], the conventional algorithm overestimates the active earth pressure distribution on the wall in the upper negative friction zone of the CFG piles.

Even though CFG pile composite foundation relatively improves the safety of the foundation pit excavation, the load redistribution and transfer mechanism in adjacent piles and the soil between piles need to be reconsidered to better understand the soil-structure interaction synergy. According to Wang and Yang [38], the load sharing phenomenon in CFG pile composite ground continues to alter throughout the process of neighbouring excavation work. The influence of excavation sequence was also studied by Fu and Li [39] using the centrifuge test, and the result indicated that the later excavation stage highly affected the load sharing characteristics of CFG piles. Physical model test results of Li et al. [40] on the load distribution of rigid-pile composite foundation revealed the same characteristics under the condition of soil displacement arising from retaining wall rotation about the base. Even though such studies highlighted the effects of soil displacement on the load bearing behaviour, they were limited to equal length piles. The current study is aimed to investigate the response of long-short pile composite foundation in immediate vicinity to retaining wall rotating about its base using numerical simulation. A large-scale indoor 1 g model test was carried out to verify the finite-element model used.

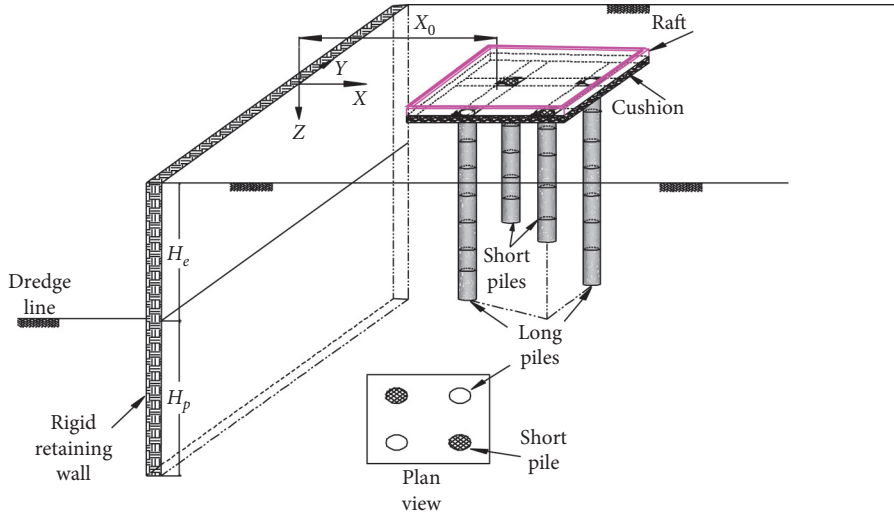


FIGURE 1: Typical nonconnected piled raft foundation near excavation.

## 2. Methodology of Analysis

**2.1. Finite-Element Modelling.** The commercial FE software ABAQUS was used to develop the finite-element model. The model comprised of structural (pile, raft, and wall) and geotechnical parts (soil and cushion) that were modelled with the elastic and elastic ideal plastic Mohr–Coulomb constitutive model, respectively. Figure 2 depicts the typical meshed geometry employed in the model. The retaining wall in each case was 10.0 m deep, to avoid boundary effects, and the homogeneously treated soil medium was made to be at least five times as wide as the breadth  $B_r$  of the raft in the lateral extent and more than three times as deep as the length of the long pile vertically.

Considering computational expenses without compromising accuracy, the mesh density was made finer in the neighbourhood of structural members with gradual change to coarser mesh sizes for farther locations. Each part was discretized using an eight-node linear brick element with reduced-integration and hourglass control (C3D8R). The surrounding vertical boundaries were modelled to restrain lateral displacements while the bottom was set to constrain both horizontal and vertical displacements. The top surface boundary was set to be free in each direction. The analysis was initiated by generating K0 geostatic stress field within the soil mass that produced very small deformation yet in equilibrium with gravity loading. This initial condition was followed by introducing sequentially piles, cushion layer, and raft by establishing surface-to-surface contacts along interacting interfaces. The face of stiffer contacting part was set as a master surface contact candidate while the face of the remaining part was described as a slave surface. Penalty friction formulation was enforced for both tangential and normal behaviour assuming 0.005 m limiting displacement for elastic slip to develop full contact friction, which overcomes overestimation of pile bending moment as suggested by Miao et al. [41].

**2.2. Verification of the Finite-Element Model.** The FE model employed in this study was compared with the results from indoor experiment conducted using a model box of  $1.6 \text{ m} \times 1.6 \text{ m} \times 2.5 \text{ m}$  inner dimension, which was sufficient to ignore boundary effects. The apparatus was designed and developed by the Research Institute of Geotechnical Engineering at Zhengzhou University. The model test setup is shown schematically in Figure 3 and comprised of stationary side walls braced with square section RHS frame; movable front wall equipped with bottom roller and slideway; and the rear wall was formed from dismountable ten split-steel plates connected to the frame with high-strength bolts. Displacement control screw rods were symmetrically located at top, middle, and lower level of the right and left edges of the front wall to permit rotation/translation in a similar way used by other researchers such as Yang et al. [42]. Rectangular RHS steel reaction frame was positioned beside sidewalls. The test was conducted on  $2 \times 2$  (2 long-2 short) pile composite foundation. Instrumented hollow aluminium close-ended tubes of length 2100 mm and 1000 mm were used as long and short piles, respectively, considering the length similarity ratio ( $\lambda_L$ ) of 3 to account for scale effect. Young's modulus of each pile was 72 GPa and was not simulated for scaling. The piles' outer diameter and thickness were 100 mm and 3 mm, respectively. The roughness of the pile shaft surface was established with knurling treatment and effected an interface angle of friction  $27.3^\circ$ . The spacing of the piles in both model and prototype was three times the pile diameter so that the area replacement ratio remains 0.087.

A plain carbon structural steel plate (quality Q235B) of dimension  $600 \text{ mm} \times 600 \text{ mm} \times 50 \text{ mm}$  was used as a rigid raft according to the stiffness requirement suggested by Horikoshi and Randolph [43]. Fine dry river sand of Zhengzhou City, China, and standard sand with the grain size distribution presented in Figure 4 were used as foundation soil and a cushion layer, respectively, in accordance with the test requirement of the Chinese specification (GB/T

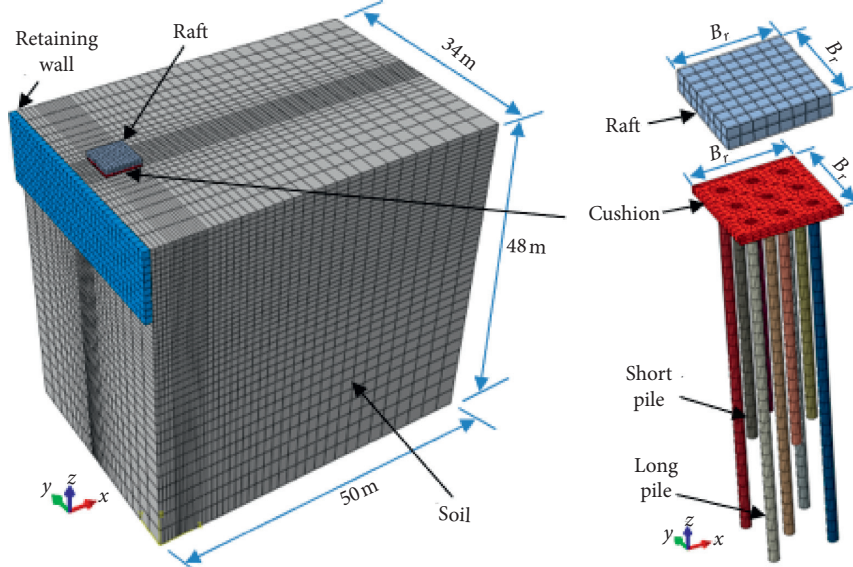


FIGURE 2: Typical three-dimensional and internal view of finite-element mesh used for 9 long-short pile composite foundation analysis.

50783-2012). The scale effect of particle size on ultimate skin friction was also cross checked to ensure the ratio of pile diameter ( $d$ ) to the average particle size of the soil ( $D_{50}$ ) was in the range 30–50 in agreement with Fioravante's [44] suggestion. The maximum and minimum dry density of the analogous fine sand was  $1.795 \text{ g/cm}^3$  and  $1.592 \text{ g/cm}^3$ , respectively. The cushion layer had a thickness of 50 mm. The bearing layer was prepared by pouring and tamping technique with the sand being freely dropped from the height of the model box by a conveyor belt. Once the fill was made to the level of the prescribed pile toe, the pile was positioned vertically and the next layer was filled up to the top surface. After the top sand surface was levelled, soil pressure cells were placed at specified locations before laying the cushion layer. After the bounding steel frame was laid, the cushion layer was placed. Then, the loading plate was stationed on top of the cushion.

The vertical working load was applied using a hydraulic jack pressed against the top beam of the reaction frame, and a load cell was mounted between the jack and beam. The model ground was given at least a week before the loading process began in order to balance the stress state of the soil. The loading application was performed according to the Chinese Technical specifications for building foundation inspection (JGJ340-2015), Technical code for testing of building foundation piles (JGJ106-2014) and Technical code for ground treatment of buildings (JGJ 79-2012).

The settlement of raft surface during the loading process was obtained from the reading taken by YHD series electronic strain type displacement sensors. All the strain gauges attached to the pile body, displacement transducers, and pressure sensors placed at the top soil surface between piles and on the head and tip of pile were all connected to static digital data acquisition system to collect real-time measurements. Each earth pressure-measuring cell and load sensor were verified for repeatability through indoor

calibration procedure preceding the experiment in order to correct calibration coefficients and stress hysteresis effect.

Based on in-house existing research works conducted with the same model box [33, 37], the top of the wall was displaced laterally an amount of  $\Delta = 10\text{--}15 \text{ mm}$  (0.47–0.75% wall height), to attain active limit state by the rotation of the wall about the base. Accordingly, this study used 10 m horizontal movement of the wall top away from the foundation in 11 stages, with 0.5 mm at the beginning and 1 mm for each of the remaining. Consequently, the displacement of the screw rods on the top were controlled manually to obtain 0.5 or 1.0 mm at each stage according to the calibration of screw rode rotation to yield the same. After the data in each stage were stable, the next rotation was carried out. Since settlement occurred as wall rotation advanced, the applied load on the foundation was manually sustained to maintain the hydraulic jack pressure unchanged throughout the process.

In order to compare experimental and numerical results, an FEA was performed on the same geometric configuration but with the depth of the sand twice the long piles' length. Table 1 summarizes material parameters used to back analyse the experiment, while Figure 5 presents the load settlement before wall rotation and the load sharing characteristics during wall rotation. It can be seen that the prediction from the numerical simulation was in agreement with the results from the experiment in terms of both magnitude and trend. Thus, the behaviour of long-short pile composite foundation can reasonably be predicted following similar numerical simulation procedure for succeeding analyses. However, there is limitation of computational results owing to the commonly applied way of contact formulation in ABAQUS software through the zero-thickness algorithm, the use of reduced-integration to take advantage of computational cost, and employing Mohr–Coulomb constitutive relationship to approximately capture the nonlinear soil behaviour. Despite these

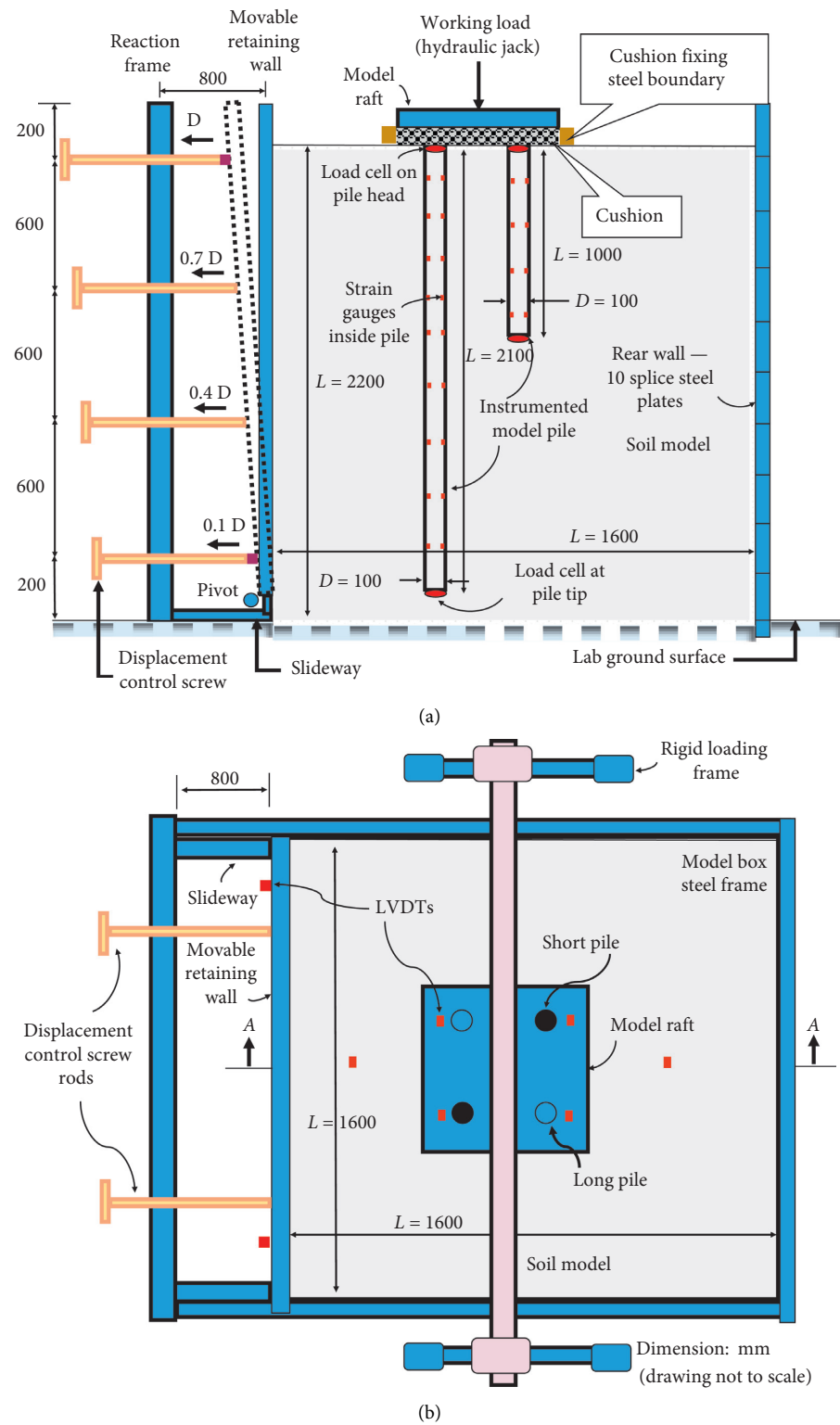


FIGURE 3: Schematic view of the test model setup: (a) sectional view and (b) plan view.

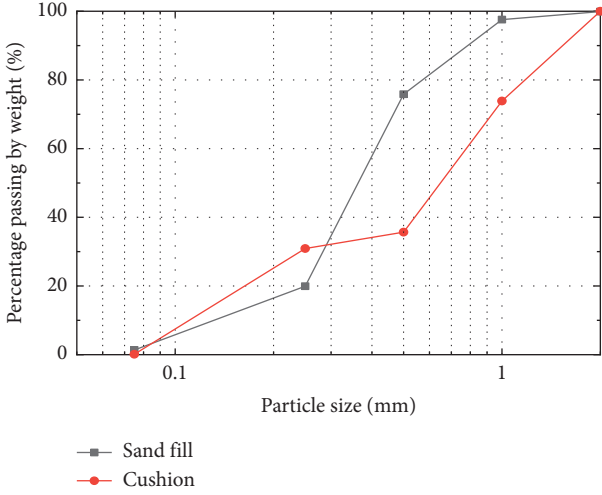


FIGURE 4: Particle size distribution of cushion and model foundation soil.

TABLE 1: Material properties used in validation.

Material type	$E$ (MPa)	$\nu$	$\gamma$ ( $\text{kg/m}^3$ )	$\Phi$ ( $^\circ$ )	$c$ (kPa)
Cushion	15.00	0.30	1416	33.90	4.00
Soil	10.50	0.30	1618	33.42	6.48
Pile	$8.14 \times 10^3$	0.20	2700	—	—
Raft	$210 \times 10^3$	0.20	7800	—	—
Retaining wall	$210 \times 10^3$	0.10	7800	—	—

limitations, robust predictions can still be made in numerical studies adopting the Mohr–Coulomb criteria and the reduced-integration formulation [9, 45, 46].

### 3. Parametric Studies

The chosen influencing factors in Table 2 were considered based on the literature on load sharing behaviour and pile responses to neighbouring excavations.

**3.1. Effect of Number of Piles.** The particular position of the pile in a group affects the response of individual piles owing to shadowing and reinforcing effect [47, 48]. The pile-soil interaction and load carrying mechanism of internal (central), lateral (edge), and corner piles are influenced by the overlapping zones of shearing resistance, which also garnered attention to use dissimilar piles for practical purposes of reducing differential settlement even in connected pile rafts [49]. Under the influence of soil movement generated because of rotating rigid retaining wall about its base, the presence of piles not only hinders the free-field soil movement to a certain level but also changes the stress state of the soil close to the piles from its already stressed condition.

As depicted in Figure 6, when the composite foundation was subjected to vertical loading of 180 kPa, increasing pile number from 4 to 25 with the same cover area ratio of 0.087 increased the load borne by long and short piles from 18.81 to 29.04% and 12.17 to 15.80%,

respectively, before commencing wall rotation. As a consequence of retaining wall rotation, the long piles' load sharing proportion increased from the earlier 18.81 to 29.04% to 22.94 to 30.34% increments at completion of wall rotation, respectively. Similarly, the percentage of load sharing for short piles has increased, but the relative increment due to number of piles was very little at the end of wall rotation, i.e., an increment of  $\leq 1\%$ . It can also be observed that the % load borne by soil between piles during progression of wall movement decreased at a higher rate for the group having four piles as compared to the other cases, indicating the behaviour of predominant pile load sharing proportion with an increasing number of piles under vertical loading results to negligible adjustment during wall rotation.

Figure 7 indicates the proportion of load carried by the central, inner, edge, and corner individual piles. Before wall rotation, the corner pile carried the highest pile head load compared to the central pile, which is in tandem with previous studies [12, 14, 50]. However, at the final rotation of the wall, the pile head load computed for shorter piles close to the wall became relatively larger and increased at a higher rate than the others while the increment for the long pile head load increased with increasing the wall rotation to a certain amount, e.g.,  $20\text{--}25 \times 10^{-4}$  rad, and then due to pile-pile interaction effect, it afterward started decreasing with the corner pile (pile A) attaining a 4% increment but the edge (pile C) 1% decrement at the end of wall rotation as compared to their initial values.

For short piles, the closer the pile (pile B) is to the wall, the greater the pile is loaded compared to the lateral pile (pile 2), inner pile (pile D), and/or rear pile (pile J). That is, at the end of wall rotation, piles B, 2, D, and J have borne 26, 22.3, 22.6, and 2% more pile head load, respectively. This is mainly attributed to the effect of reduction in load bearing contribution from the soil between piles due to wall rotation-induced soil settlement.

Moreover, the stress on long piles' top is greater than that on the short piles throughout wall rotation process (Figure 6). Owing to the group effect, the load shared by the front and inner short piles keeps increasing with an increasing number of piles while the edge short piles gradually stabilize their share in a steady manner to accommodate the soil bearing capacity reduction. In other words, this increase in the piles' load sharing can be interpreted as the piles' bearing capacity loss because the piles act as if they are subjected to a new loading condition violating the settlement criteria due to the effect of the induced soil movement. Such "apparent loss of pile capacity" happened due to external soil displacement, and the induced extra pile settlement can be correlated to describe the bearing capacity loss of existing piles in a similar concept as the routinely used settlement criteria for pile failure (settlement due to degradation of shear stiffness rather than "bulb stress"), which however does not necessarily mean it affects the ultimate geotechnical load bearing capacity of piles. Therefore, due diligence should be given to avoid or reduce the adverse effect on the structural integrity [19, 51].

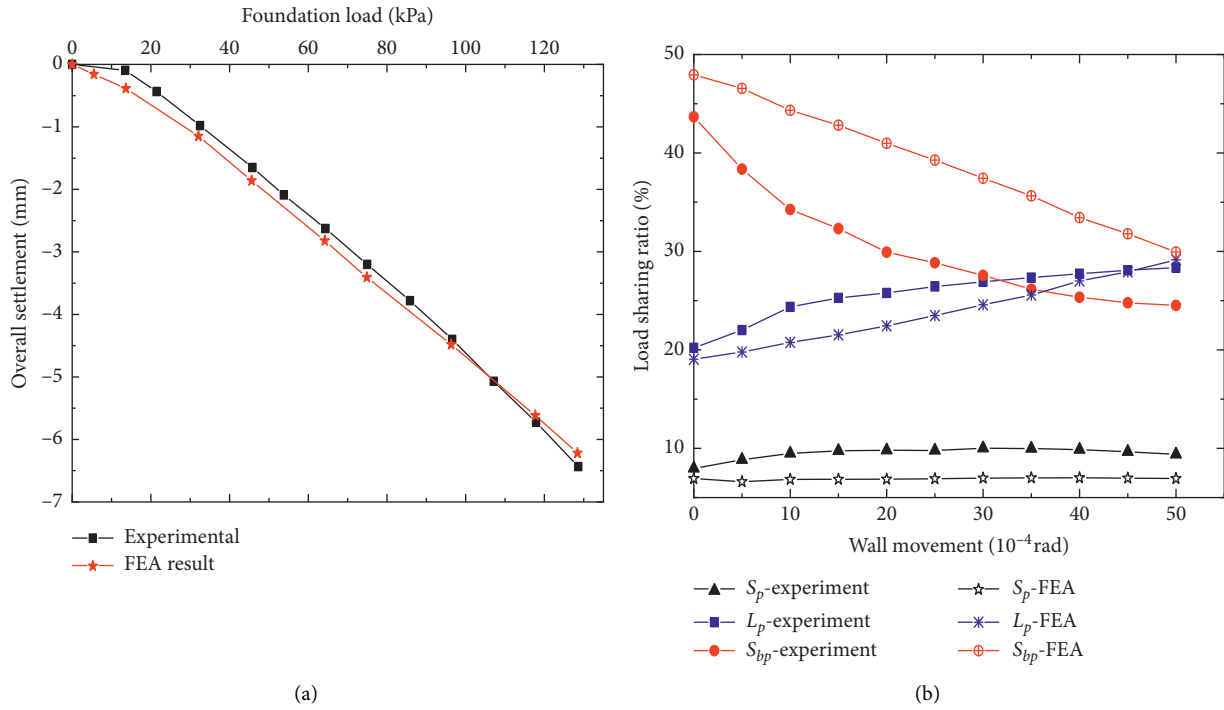


FIGURE 5: Comparison of experimental (a) load settlement curve and (b) load sharing ratio during wall rotation with finite-element analysis result ( $L_p$ : long pile,  $S_p$ : short pile, and  $S_{bp}$ : soil between piles).

**3.2. Effect of Pile Spacing.** For passive piles that are arranged in a group with closer pile spacing, the increase in spacing increases the lateral soil movement-induced forces acting on them due to soil arching phenomenon. Beyond the spacing of 8 times the pile diameter, the group effect and arching would not be felt, and the failure mode of the soil surrounding the piles would be the same as that of a single pile [48]. In composite pile foundation, pile spacing directly reflects one of the basic load sharing parameters, the pile area replacement ratio,  $m$ . Apart from changing the spacing, the area replacement ratio can also be varied by increasing the diameter of the pile (or its head) [50, 52, 53] and/or provision of pile cap [54, 55]. From the mechanical characteristics of CFG pile composite foundation, it is well known that the smaller the clearance between neighbouring piles, the larger the cover ratio of piles and the smaller the load sharing proportion of the soil, meanwhile reducing the foundation settlement. For piles of diameter  $d$  arranged in a group with a square configuration of spacing  $s$ , it is common to describe the area replacement ratio using

$$m = \frac{(\pi d^2 / 4)}{s^2} \quad (1)$$

As predictable from the characteristics of composite foundation under vertical loading, the lower the area replacement ratio, the lower the soil load sharing proportion in the initial stage (see Figure 8). Provoking wall rotation only increases the pile load sharing proportion, keeping the trend almost similar, in an attempt to equilibrate the additional load impinged by soil stress release from imposed soil movement.

Comparing the effect of replacement ratio on the load sharing proportion of soil between piles during the progression of wall movement, it is observed that the percentage load transmitted to the soil beneath the cushion layer reduces at a higher rate for the group with larger pile spacing than the configuration with smaller spacing between piles. What is understandable also is that as the area replacement ratio is increased (and gradually approaches the optimal pile area cover), the more favourably it contributes to the settlement and bearing capacity enhancement of the whole composite ground; consequently, it makes the composite ground stiffer so that its load sharing mechanism is less disturbed. The larger the number of piles that are stiffer than the surrounding soil, the better the performance in reducing the upcoming decrease in bearing capacity from wall movement-induced soil displacements.

**3.3. Effect of Pile Tip Location.** Assessing earlier research indicates that increasing the ratio of long to short pile length for a given length of long pile increases the pile-soil stress ratio of the short pile while reducing the same for the long piles [56]. On the other hand, the formation level of excavation with respect to the depth of pile tip affects the response of pile to neighbouring excavation [51], and for short piles as compared to long ones, excavation-induced pile settlement is likely to be a significant factor than lateral pile deflections [21]. Akin to the stress release attributable to excavation, wall movement-induced deformation of soil leads to reduction in pile-soil stiffness, which in turn brings pile settlement owing to degradation of pile-soil interface stiffness and changes in pile-soil load sharing ratio.

TABLE 2: Details of the parametric studies.

Parameter	Raft dimensions		Cushion parameter		Subsoil parameter			Pile group geometry			Working load	
	$B_r \times L_r \times t_r$ (m)	$t_c$ (m)	$E$ (MPa)	$\phi$ ( $^{\circ}$ )	$E$ (MPa)	$\phi$ ( $^{\circ}$ )	$n_p$	$S_p/d_p$	$X_0$ (m)	$L_{sp}$ (m)	$L_{lp}$ (m)	(kPa)
Number of piles, $n_p$	$2.8 \times 2.8 \times 0.8$							4				
	$4.0 \times 4.0 \times 0.8$	0.3	15.0	33.9	10.0	31.0	9	16	3	3	10.0	15.0
	$5.2 \times 5.2 \times 0.8$							25				
	$6.4 \times 6.4 \times 0.8$											
Pile spacing, $S_p$	$4.0 \times 4.0 \times 0.8$							3				
	$4.8 \times 4.8 \times 0.8$	0.3	15.0	33.9	10.0	31.0	9	4	3	3	10.0	15.0
	$5.6 \times 5.6 \times 0.8$							5				
Pile length, $L_p$	$4.0 \times 4.0 \times 0.8$	0.3	15.0	33.9	10.0	31.0	9	3	3	10.0	15.0	180
										6.0	10.0	
										15.0	15.0	
										15.0	20.0	
Cushion stiffness, $t_c$	$4.0 \times 4.0 \times 0.8$	0.3	60.0	33.9	10.0	31.0	9	3	3	10.0	15.0	180
			90.0									
			120.0									
Cushion thickness	$4.0 \times 4.0 \times 0.8$	0.5	15.0	33.9	10.0	31.0	9	3	3	10.0	15.0	180
		0.6										
		0.7										
Subsoil stiffness	$4.0 \times 4.0 \times 0.8$	0.3	15.0	33.9	10.0	31.0	9	3	3	10.0	15.0	180
			15.0									
			18.5									
Distance from wall, $X_0$	$4.0 \times 4.0 \times 0.8$	0.3	15.0	33.9	10.0	31.0	9	3	7.5	10.0	15.0	180
			10									
			15									
Applied working load on raft	$4.0 \times 4.0 \times 0.8$	0.3	15.0	33.9	10.0	31.0	9	3	3	10.0	15.0	180
			350									
			500									
			700									
			900									

Remark. E: elastic modulus, B: breadth,  $L_{sp}$ : short pile length,  $L_{lp}$ : long pile length, and dilation angle ( $\psi$ ) was taken as  $\psi = \phi - 30^{\circ}$ .

Alongside it, when floating piles are subjected to both axial load on pile head and a surcharge on top of the surrounding soil, the relative pile-soil settlement characteristics and the down-drag load on the piles are affected by the location of pile tip relative to the stable and/or firm stratum [57]. In this section, in order to demonstrate the influence of pile tip location, the length of short piles is varied whereby the pile toe is positioned above, at and below the depth of axis of wall rotation.

Figure 9(a) shows the lateral deflection of selected piles. It demonstrates that the horizontal displacement and deflection of short pile positioned above the depth of axis of wall rotation are greater than the computed results for piles located at and below it. In addition, the longer the piles, the more slender they become and the pattern of deflection profiles follows a similar response like the relatively flexible semirigid conventional piles. Moreover, the longer the pile, the larger its

lateral head displacement. However, for short piles, the lateral pile toe displacement is far larger than the long pile's tip horizontal displacement, and it is more pronounced for the pile tip located above the depth of axis of wall rotation. At first glance, it is apparent that both the head and tip of short piles undergo a certain amount of translation and rotation while the base of the 20 m long piles encounter restraint boundary condition from the surrounding soil. It is also important to note that rear pile experiences smaller translation and deflection than front pile along the same axis.

At the end of the wall rotation, as can be observed from Figure 9(b), irrespective of the pile tip location, the maximum positive bending moment induced in the front corner pile close to the wall is greater than that of the central and rear corner piles. The axial strains at the outermost nodes of the pile are used to calculate the bending moment distribution,  $M(z)$ , at any depth  $z$  from the pile top according to

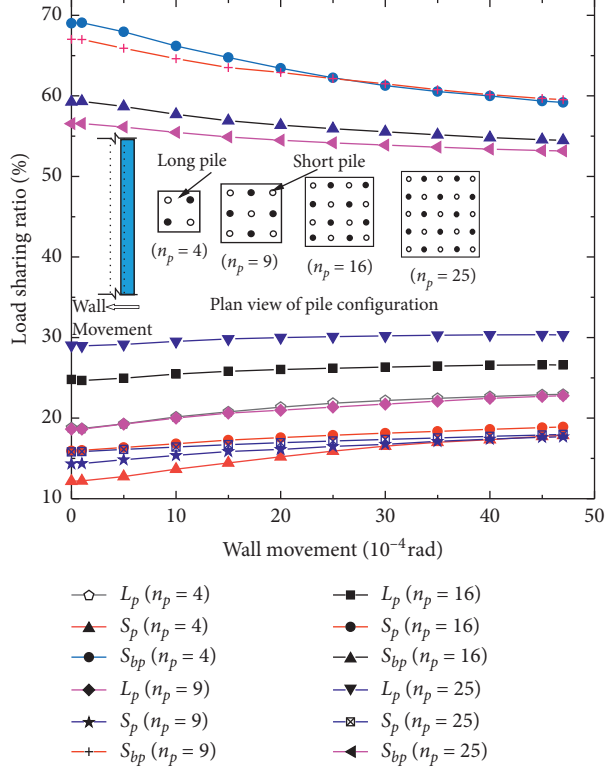


FIGURE 6: Influence of number of piles on the change in pile/soil load sharing ratio of the composite foundation located at 3.0 m behind the rotating wall.

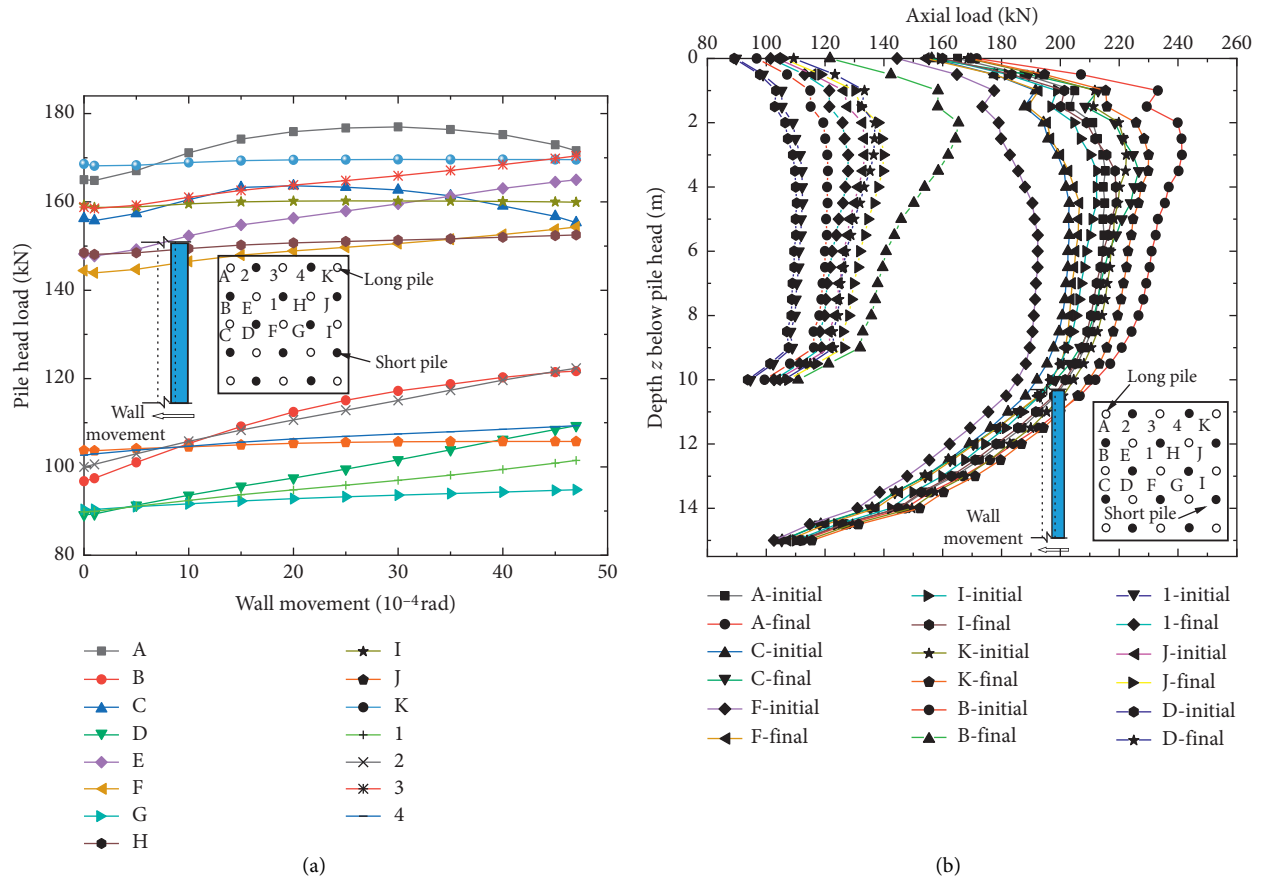


FIGURE 7: Wall rotation-induced variation of (a) pile head load and (b) axial load distribution in 5×5 long-short pile group located at 3 m away from the wall.

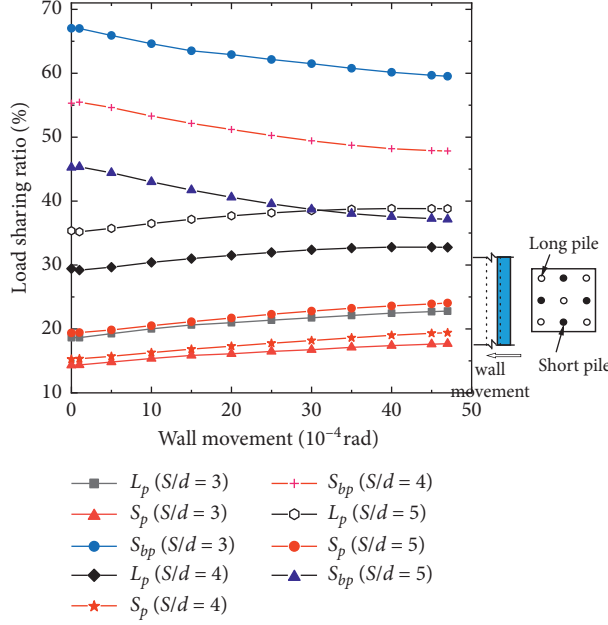


FIGURE 8: Variation of pile/soil load sharing proportion with pile spacing during wall rotation.

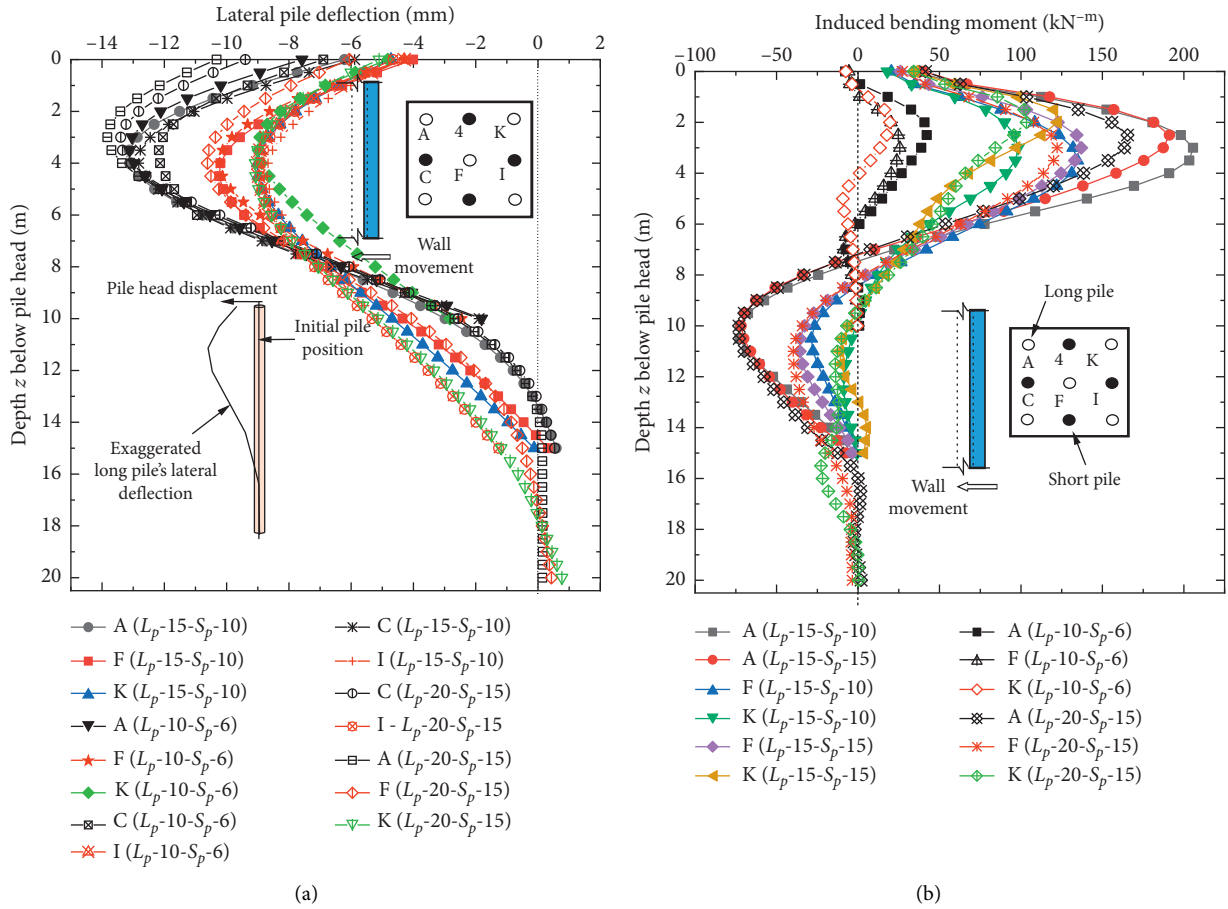


FIGURE 9: Influence of pile length on (a) deflection profile and (b) bending moment induced along the length of long piles.

$$M(z) = \frac{E_p I_p (\varepsilon_1 - \varepsilon_2)}{2r}, \quad (2)$$

where  $E_p$  is Young's modulus of the pile,  $I_p$  is the moment of inertia of the pile,  $\varepsilon_1/\varepsilon_2$  are the axial strains along the compression and tension face of pile shaft at the depth  $z$  on both sides of neutral axis, and  $r$  is the radius of the pile. For convenience, the bending moment is considered positive for the induced tensile stress facing towards the retaining wall.

It can also be demonstrated from Figure 9 that letting the length of short piles to be equal to that of the long piles (i.e., both piles assume the same length: 15 m) decreases the maximum bending moment induced in the front peripheral pile of the long-short pile (long 15 m and short 10 m long) placed at the same location. Moreover, owing to the influence of the surrounding reinforcing piles (also affected by distance from wall), the group interaction effect makes the edge and middle piles experience less exposure to disturbance from soil movement and hence the smaller the induced bending moment along them as compared to the peripheral ones but with similar trend. For instance, if the group having 15 m long piles and 10 m short piles is taken, the shielding effect resulted in a 53% and 109% higher bending moment in the front long pile (pile A) as compared to that of the bending moment developed in the central (pile F) and rear corner pile (pile K), respectively, whereas the rear short pile (pile I) sustained a bending moment 53% less than that of the short pile adjacent to the wall (pile C).

Consistent with the difference in displacement of short piles for each case and further pile settlement to mobilize additional pile tip and shaft resistance, the change in pile load sharing ratio of the group of piles with short piles at and above the depth of wall rotation axis is different from that located below it. Figure 10 shows that the rate at which the % load proportion carried by the soil between piles reduces is greater for short piles placed at closer depth to the slip surface (i.e., short piles at and above the depth of axis of wall rotation) than that at a deeper position because of the resultant soil disturbance acting on larger portion of the pile body. Accordingly, the percentage load increment received by long piles increases at higher rate in the composite foundation with short piles of length 6 and 10 m than that of 15 m. Observable from Figure 10 is that the larger the length of piles, the more the load transferred.

**3.4. Effect of Subsoil Stiffness.** Increase in soil stiffness decreases excavation-induced bending moment and horizontal deformation of nearby piles [58]. It also affects pile's response under vertical loading [53, 59]. In addition, it is apparent that the compressibility characteristics of the subsoil depends on its stiffness and affects the pile-soil relative settlement, hence influencing the load sharing characteristics of a composite foundation.

As illustrated in Figure 11, piles embedded in a soil of lower Young's modulus take larger proportion of load and the % load carried by the soil does not drop as rapidly as observed in higher stiffness soils. On the other hand, the stiffer the interposed soil, the smaller the imposed load

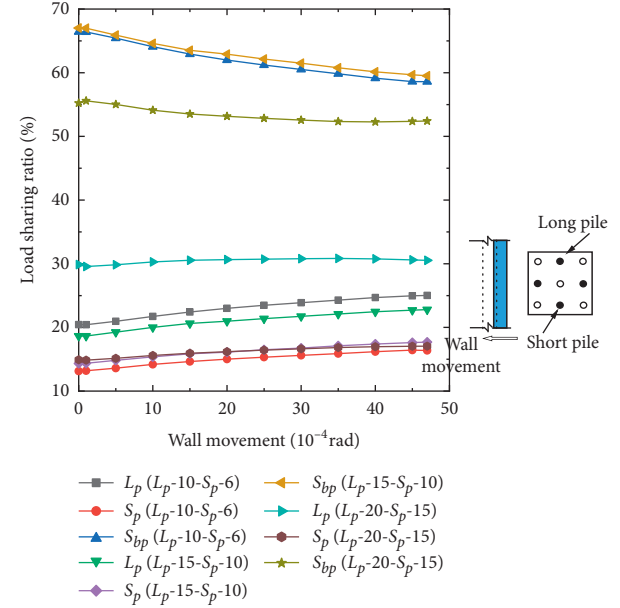


FIGURE 10: Load sharing proportion during wall rotation for short pile tip located above, at, and below the axis of wall rotation.

proportion of the piles; that is, it exhibits an inverse relationship, and as the wall movement progresses, the % load received by the piles increases at a comparatively higher rate until a wall rotation value of  $30 \times 10^{-4}$  rad and begins to be relatively moderate. The higher the modulus of the subsoil between piles, the larger the load percentage the soil shares prior to wall rotation, and the mobilized bearing capacity reduction in the process of wall rotation increases the concentration of stresses on the CFG piles at a higher rate than the increment for piles installed in soils with lower modulus. The larger the value of subsoil Young's modulus, the smaller the soil displacement due to wall rotation (also explained by [60]) and the larger the stress borne by the soil between the piles. In spite of the small soil displacement in the earlier wall rotation, there is a significant reduction in the load taken by the shallow soil between piles.

**3.5. Effect of Stiffness and Thickness of Cushion.** The variation of load sharing ratio for different cushion thickness and stiffness values during progression of wall rotation is depicted in Figure 12. In the interest of foundation load fine-tuning ability of the interposed layer, a higher modulus of elasticity of the cushion changes the percentage of the load transferred to piles appreciably in the earlier stage of wall rotation (i.e., up to  $15 \times 10^{-4}$  rad). Subsequently, in the mentioned wall rotation, the load sharing percentage of the soil decreases at larger rate, and beyond that point both piles and soil attain almost uniform load redistribution except for the case of the 15 MPa cushion. Nevertheless, from the load sharing ratio curves of varying cushion thickness in Figure 12(b), it is evident that there is a higher % load sharing ratio of soil between piles for lower cushion thickness which decreases with increase in thickness until completion of wall rotation.

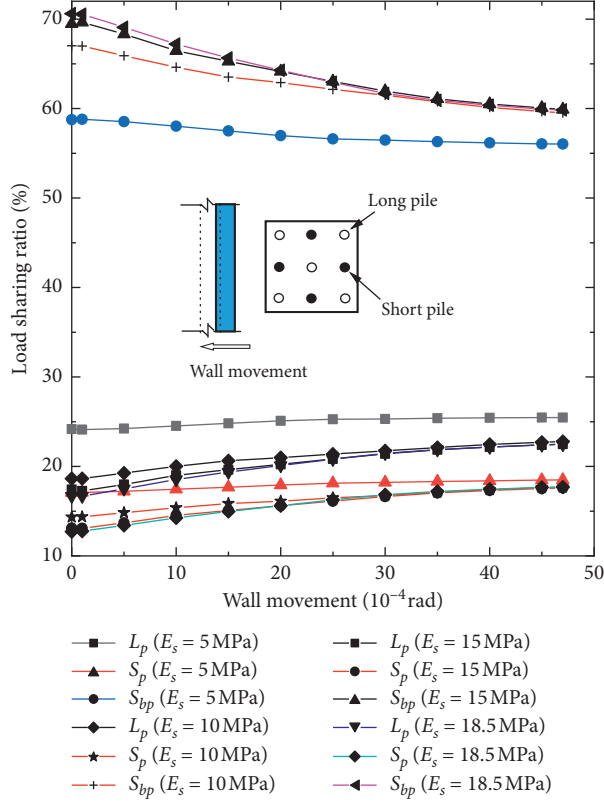


FIGURE 11: Influence subsoil stiffness on load sharing ratio of 9 long-short pile composite foundation configuration.

**3.6. Effect of Location Away from the Wall.** The pile position in a group and its perpendicular distance from the retaining wall are among the important factors affecting the response of pile groups to imposed soil displacements [45, 61]. Therefore, it was sought to give insight on the influence of the same in CFG pile composite foundations. Besides, with the increase of retaining wall rotation, the soil behind the retaining wall tends to move, and then the soil between the piles settles so that the upper load is gradually transferred to the pile top. The triggered soil displacement field behind the wall diminishes as the distance from the supporting structure increases, and so it does the soil settlement along the depth. In line with the largest ground displacement near the wall, the expected maximum lateral pile deflection occurs around its head [62]. In this regard, it is common to consider the tolerance to soil displacement of neighbouring structures located within the “Apparent excavation Influence Range (AIR)” [63, 64]. Unsurprisingly, Figure 13 shows that the incident of proceeding wall movement affects very little the load sharing proportion of CFG pile composite foundation placed at far distance as compared to those which are closer to the wall. In fact, owing to the cushion’s stress diffusive mechanism that produces uneven stress distribution

between the pile and soil under vertical loading condition, bending moments are generated at different places of the pile body before wall rotation, but the bending moment value is mostly small.

Figure 14 shows the bending moment profile of short and long piles at various distance  $x_0$  away from the retaining wall for a group of 9 piles. Interestingly, it was observed that increasing  $x_0$  from 3.0 m to 15.0 m decreases the maximum bending moment developing both in long and short piles in a similar pattern, except for the cases where curvature deviates for the piles at far distance whose considerable pile body lies outside the theoretical failure zone, such as Rankine’s slip surface. In addition, the farther the group is located away from the retaining structure, the farther its centroid shifts away from the back face of the wall and experiences lesser wall rotation-induced soil displacements, and in turn a lesser pile deflection of the group as a whole. This is consistent with the decrease in soil deformation zone for locations away from the retaining wall so that the decrease in shear strain magnitude will not weaken the majority of the surrounding soil confining the rear piles, whereby the smaller the pile proportion within the disturbed soil mass, the lower the bending moment.

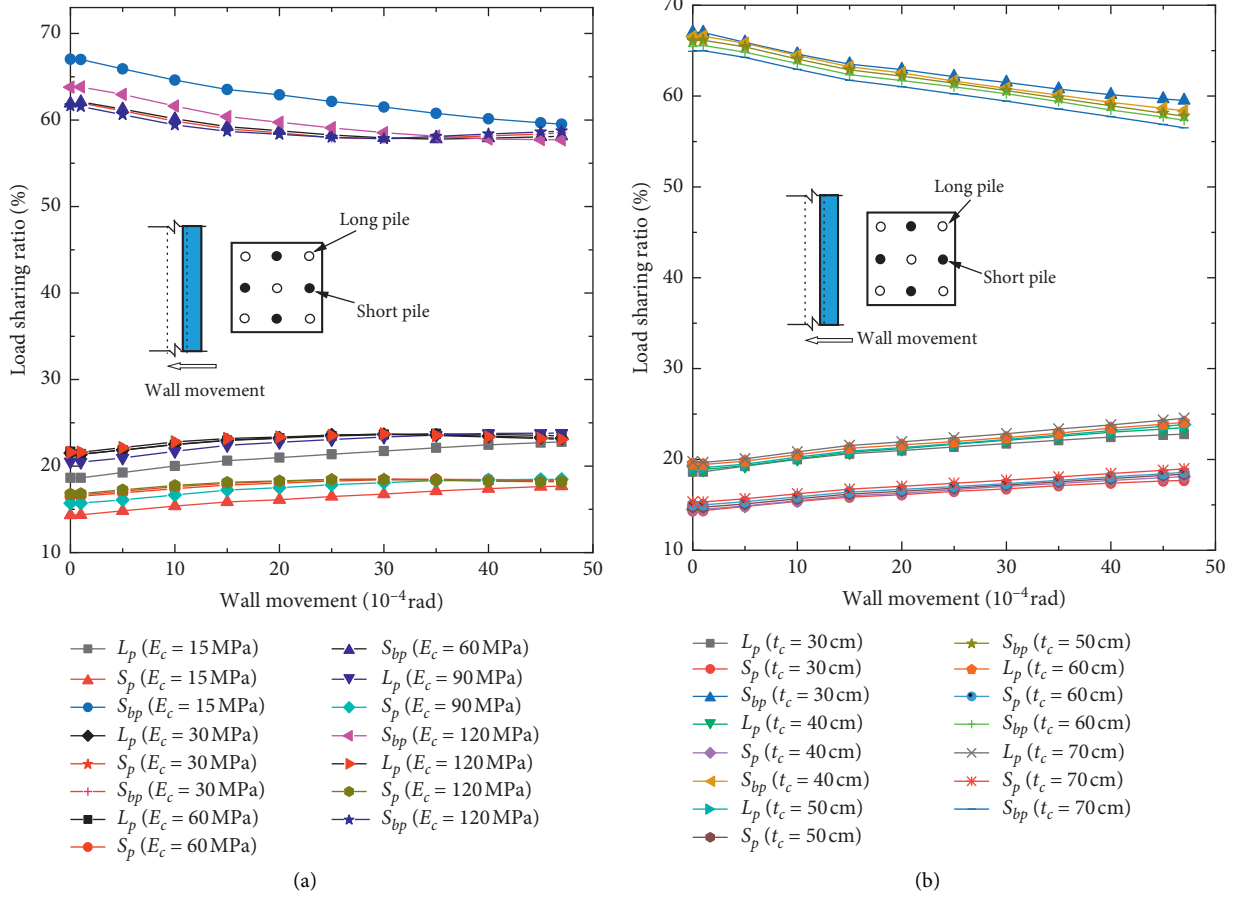


FIGURE 12: Effect of cushion's (a) elastic modulus and (b) thickness on the load sharing behaviour of 9 long-short pile composite foundation.

Having in mind the reduction of pile axial load carrying capacity as excavation-induced bending moment increases [58, 65], sudden structural failure by bending can be prevented by assessing whether or not the pile's section yield moment is exceeded. Moreover, since CFG piles are usually unreinforced, the possibility of developing sever cracks due to the induced bending moment may cause lateral bearing capacity loss, which would affect the cooperation and integrity of the CFG piles in the group. In the conventional pile group back-analysis using excavation-induced free-field soil movement, it is recommended to take into account pile moment of inertia deterioration to avoid overconservative structural pile responses corresponding to the pile cracking bending moment for large soil displacements at fully mobilized active lateral soil stresses [66, 67]. In this regard, it is often the horizontal component of excavation-induced soil movement and the associated large lateral pile displacement recognized to be more crucial for adjacent concrete piles [68, 69]. One can also notice at this point that the further the rear piles are located from the wall, the lesser the soil movement experienced by the piles and consequently the lesser the pile deflection. This puts the piles in a relatively more stable situation as compared to the soil dragging action impinged on the front row piles. The peripheral CFG piles, especially those close to the wall, experience larger bending

moment as compared to the middle piles in each row, which may need special attention to confirm whether or not the section's capacity is exceeded under a given working load.

**3.7. Effect of Applied Working Load.** The intensity of foundation load has been reported to have negligible impact on the lateral reaction of conventional pile to excavation-induced soil movements [58, 65] but significantly affects its settlement behaviour [70, 71]; hence, owing to the distinct feature of relative pile-soil settlement in composite foundation, observation was sought to assist shed more light on the effect of higher stress level encountered prior to introducing wall rotation-induced soil movement.

Figure 15 shows the increase in % load sharing ratio of piles with increase in the applied foundation load preceding wall movement, which is a trend in agreement with the pile-soil stress ratio characteristics of composite foundations. The bigger the applied working load, the larger the load carried by the piles and the smaller the proportion of load borne by the upper soil. As the wall movement proceeds, the reduction of % load share in the soil and the increment in both long and short piles occur following a moderate trend but with fairly higher change for lower working load applied on the raft. It can also be seen from the axial force distribution along the

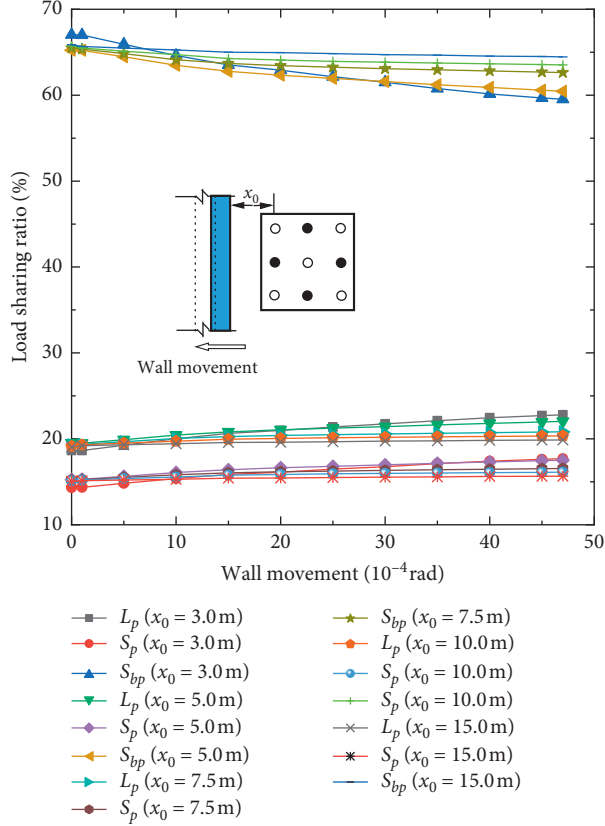


FIGURE 13: Influence of distance away from wall on load sharing proportion in the process of wall rotation.

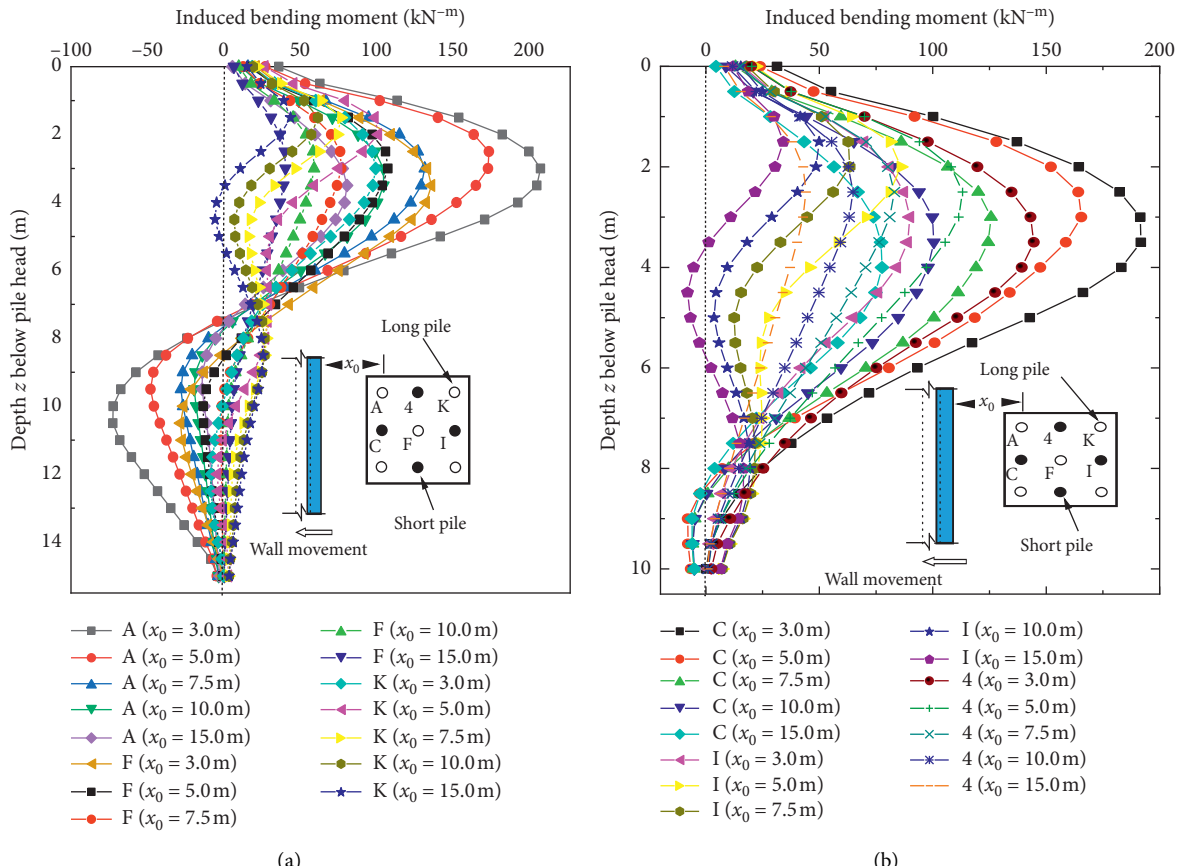


FIGURE 14: Bending moment profiles of (a) long piles and (b) short piles at different distances from wall after completion of wall rotation.

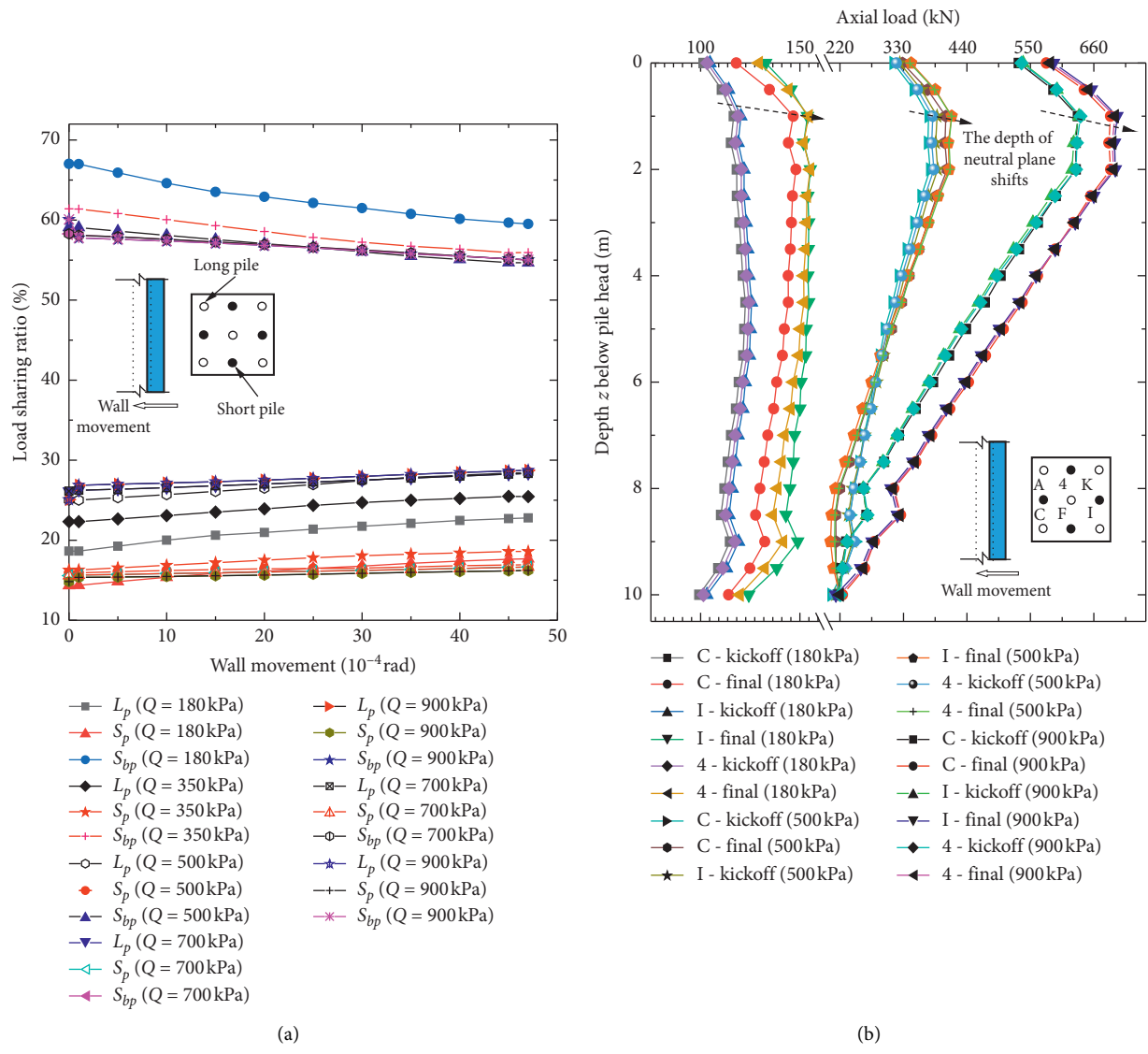


FIGURE 15: Continued.

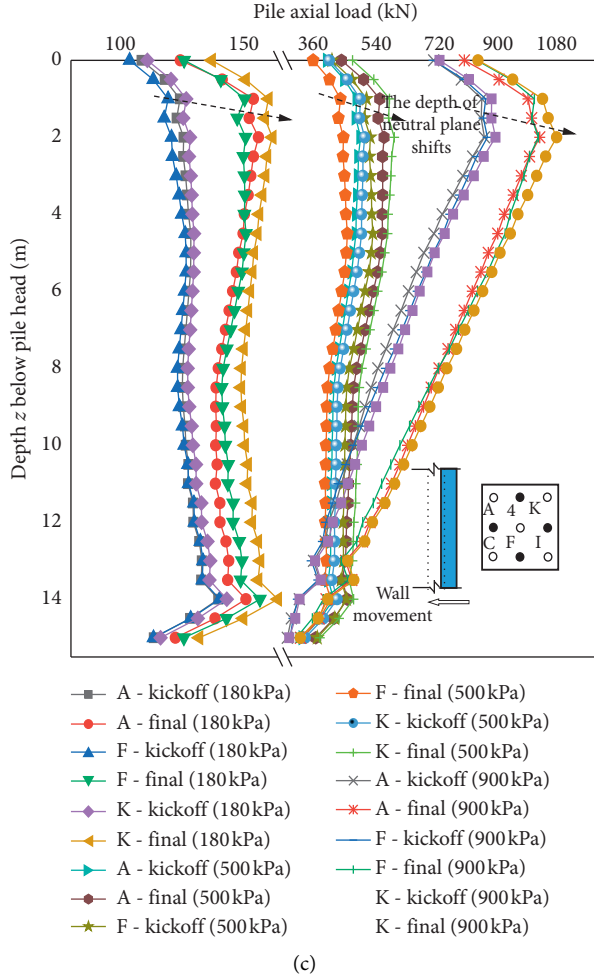


FIGURE 15: Effect of working load intensity during wall rotation on (a) load sharing ratio and (b) short and (c) long pile axial load distribution in  $3 \times 3$  long-short pile group located at 3 m away from the wall.

pile length that the neutral plane where the maximum normal force happens to exist shifts downwards due to the soil movement-induced relative pile-soil settlement.

#### 4. Conclusion

In this article, 3D finite element modelling was established based on 1g large-scale experiment to investigate the influence of retaining wall rotation on the load sharing behaviour of adjacent long-short CFG pile composite foundation. The following conclusions were drawn:

- (i) The process of wall rotation about the base increased the displacement of the soil near the wall, and the anticipated soil movement decreased with increase in depth and distance away from the wall. The prompted soil settlement associated with progression of wall movement resulted in continuous reduction of the mobilized bearing capacity of the soil between piles. The soil bearing capacity loss for the composite foundation having 9 long and short piles range was 1.4–7.5% of the total imposed load depending on how far the foundation was situated away from the wall.

Consequently, the percentage load sharing of piles increased, ranging between 0.83–4.15 and 0.59–3.36%, respectively, for the long and short piles depending on the location of the foundation behind the wall, as the proportion of the subsequent decrease in stress borne by the soil between piles transferred to the piles.

- (ii) During wall rotation, the 3D soil movement behind the wall increased the vertical and lateral soil strain near the wall. As the soil elements near the wall were subjected to larger principal strain increments with near-lateral extension, it led to larger stress relief experienced by front piles in comparison to the piles far away from the wall. On the other hand, the lateral displacement experienced by the soil between piles with higher elastic modulus was smaller than the soil with low stiffness but as it bore higher load proportion prior to wall rotation, significant reduction in the load taken by the soil was observed more in the earlier wall rotation, i.e., up to  $15 \times 10^{-4}$  rad. For the composite foundation having 9 long and short piles placed at 3.0 m behind the

- wall, the soil bearing capacity drop observed was 10.77 and 2.73% of the imposed load for the subsoil elastic modulus of 18.5 and 5 MPa, respectively.
- (iii) Depending on the pile tip location with respect to the failure surface, the pile lateral response varied. The proportion of the pile body intersected by the slip line and its embedded depth in the stable layer influenced the reaction of the pile to the soil movement.
  - (iv) During wall rotation progression, the increment in proportion of the load taken by each pile varied depending on the position of the piles in the group and the adjacent wall. The contribution of short piles increased during the course of wall rotation. For the composite foundation having 25 long and short piles placed at 3 m behind the wall, the front long pile attained 4% pile head increment while the short pile bore as much as 26% more head load as compared to the 2% rear short pile's head load increment. Peripheral piles and those close to the wall received the highest load.
  - (v) For each key factor chosen, long piles' load sharing proportion was bigger than that of the short piles. The larger the area replacement ratio, the more it improved the vertical bearing capacity and the lesser the disturbance in percentage of load shared by the piles and the soil during wall rotation compared to the group with smaller area replacement ratio.

## Data Availability

The data used to support the findings of this study are available from the corresponding author upon request.

## Conflicts of Interest

The authors declare that there are no conflicts of interest regarding the publication of this paper.

## Acknowledgments

This work was supported by the National Natural Science Foundation of China (51508522).

## References

- [1] B. U. Uge and Y.-C. Guo, "CFG pile composite foundation: its engineering applications and research advances," *Journal of Engineering*, vol. 2020, Article ID 5343472, 26 pages, 2020.
- [2] J. Han, "Recent research and development of ground column technologies," *Proceedings of the Institution of Civil Engineers-Ground Improvement*, vol. 168, no. 4, pp. 246–264, 2015.
- [3] P. Halder and B. Manna, "Large scale model testing to investigate the influence of granular cushion layer on the performance of disconnected piled raft system," *Acta Geotechnica*, vol. 16, no. 5, pp. 1597–1614, 2021.
- [4] R. Rui, J. Han, Y. Ye, C. Chen, and Y. Zhai, "Load transfer mechanisms of granular cushion between column foundation and rigid raft," *International Journal of Geomechanics*, vol. 20, no. 1, Article ID 04019139, 2020.
- [5] W. Jiang and Y. Liu, "Determination of neutral plane depth and pile-soil stress ratio of the rigid pile composite foundation," *Rock and Soil Mechanics*, vol. 39, no. 12, pp. 4554–4560, 2018.
- [6] F. Tradigo, F. Pisanò, and C. Di Prisco, "On the use of embedded pile elements for the numerical analysis of disconnected piled rafts," *Computers and Geotechnics*, vol. 72, pp. 89–99, 2016.
- [7] C. Wu, W. Guo, and Y. Li, "Calculation of neutral surface depth and pile-soil stress ratio of rigid pile composite foundation considering influence of negative friction," *Chinese Journal of Geotechnical Engineering*, vol. 38, no. 2, pp. 278–287, 2016.
- [8] V. Fioravante and D. Giretti, "Contact versus noncontact piled raft foundations," *Canadian Geotechnical Journal*, vol. 47, no. 11, pp. 1271–1287, 2010.
- [9] A. Ata, E. Badrawi, and M. Nabil, "Numerical analysis of unconnected piled raft with cushion," *Ain Shams Engineering Journal*, vol. 6, no. 2, pp. 421–428, 2015.
- [10] F.-X. Yan and X.-Z. Huang, "Experiment research of bearing behavior on lime-soil pile and CFG pile rigid-flexible pile composite subgrade," in *Proceedings of the Ground Improvement and Geosynthetics). GeosyntheticsPresented at the Geo-Shanghai 2014*, pp. 40–48, American Society of Civil Engineers, Shanghai, China, May 2014.
- [11] E. Zhang, L. Yu, and X. He, "Analysis of action mechanism for rigid flexible pile composite foundation," *Revista Técnica de la Facultad de Ingeniería Universidad del Zulia*, vol. 39, no. 11, pp. 260–270, 2016.
- [12] Y. C. Guo, S. H. Zhang, G. Shi, and N. Liu, "Optimization strategy of the long-short-pile composite foundation based on the settlement control," *Advanced Materials Research*, vol. 243–249, pp. 2429–2434, 2011.
- [13] H. Lu, Q. Gao, B. Zhou, D. Wang, and M. Liang, "Experimental research on bearing capacity of long-and-short pile composite foundation," *Chinese Journal of Underground Space and Engineering*, vol. 11, pp. 56–63, 2015.
- [14] X. Xinsheng Ge, X. Xiaoli Zhai, J. Jiangwei Xue, and X. Xiaohong Bai, "Model test study of impact of pile length on long-short piles composite foundation," in *Proceedings of the 2011 International Conference on Electric Technology and Civil Engineering (ICETCE)*, pp. 2370–2374, IEEE, Lushan, China, April 2011.
- [15] V. J. Sharma, S. A. Vasavada, and C. H. Solanki, "Behaviour of load-bearing components of a cushioned composite piled raft foundation under axial loading," *Slovak Journal of Civil Engineering*, vol. 22, no. 4, pp. 25–34, 2014.
- [16] J.-J. Zheng, S. W. Abusharar, and X.-Z. Wang, "Three-dimensional nonlinear finite element modeling of composite foundation formed by CFG-lime piles," *Computers and Geotechnics*, vol. 35, no. 4, pp. 637–643, 2008.
- [17] Y. Guo, C. Lv, S. Hou, and Y. Liu, "Experimental study on the pile-soil synergistic mechanism of composite foundation with rigid long and short piles," *Mathematical Problems in Engineering*, vol. 2021, Article ID 6657116, 15 pages, 2021.
- [18] T. Ma, Y. Zhu, X. Yang, and Y. Ling, "Bearing characteristics of composite pile group foundations with long and short piles under lateral loading in loess areas," *Mathematical Problems in Engineering*, vol. 2018, Article ID 8145356, 17 pages, 2018.
- [19] H. G. Poulos, "Ground movements-a hidden source of loading on deep foundations," *DFI Journal: the Journal of the Deep Foundations Institute*, vol. 1, no. 1, pp. 37–53, 2007.
- [20] X.-J. Zhu, K. Fei, and S.-W. Wang, "Horizontal loading tests on disconnected piled rafts and a simplified method to

- evaluate the horizontal bearing capacity," *Advances in Civil Engineering*, vol. 2018, Article ID 3956509, 12 pages, 2018.
- [21] M. Korff, R. J. Mair, and F. A. F. Van Tol, "Pile-soil interaction and settlement effects induced by deep excavations," *Journal of Geotechnical and Geoenvironmental Engineering*, vol. 142, no. 8, Article ID 04016034, 2016.
- [22] M. Li and J. Zhao, "Progress of research advance on the model tests on the interaction between new constructions and adjacent existing buildings," in *Proceedings of GeoShanghai 2018 International Conference: Tunnelling and Underground Construction*, D. Zhang and X. Huang, Eds., Springer, Singapore, Asia, pp. 536–547, 2018.
- [23] L. Mu, W. Chen, M. Huang, and Q. Lu, "Hybrid method for predicting the response of a pile-raft foundation to adjacent braced excavation," *International Journal of Geomechanics*, vol. 20, no. 4, Article ID 04020026, 2020.
- [24] B. U. Uge and G. Y. Cheng, "Research Progress on the influence of deep foundation pit excavation on adjacent pile foundation," in *Proceedings of the Ninth International Conference on Advances in Civil, Structural and Mechanical Engineering CSM-2019*, pp. 12–19, Institute of Research Engineers and Doctors, Rome, Italy, December 2019.
- [25] H. Zhou and H. Zhang, "Risk assessment methodology for a deep foundation pit construction project in Shanghai, China," *Journal of Construction Engineering and Management*, vol. 137, no. 12, pp. 1185–1194, 2011.
- [26] J. Chai, S. Shen, W. Ding, H. Zhu, and J. Carter, "Numerical investigation of the failure of a building in Shanghai, China," *Computers and Geotechnics*, vol. 55, pp. 482–493, 2014.
- [27] Z. Xiong, H. Lu, M. Wang, Q. Qian, and X. Rong, "Research progress on safety risk management for large scale geotechnical engineering construction in China," *Rock and Soil Mechanics*, vol. 39, no. 10, pp. 3703–3716, 2018.
- [28] M. Korff, *Geotechnical Aspects of Underground Construction in Soft Ground*, A. Negro and M. O. Cecilio, Eds., CRC Press, Boca Raton, FL, USA, 1st edition, 2017.
- [29] C. O'Neil, "Effective risk management processes," *Global Construction Success*, John Wiley & Sons, Chichester, UK, 1st edition, 2018.
- [30] B. Uba Uge and Y. Guo, "Deep foundation pit excavations adjacent to disconnected piled rafts: a review on risk control practice," *Open Journal of Civil Engineering*, vol. 10, no. 3, pp. 270–300, 2020.
- [31] National Standard of the People's republic of China (JGJ 79–2012), *Technical Code for Ground Treatment of Buildings*, China Architecture & Building Press, Beijing, China, 2012.
- [32] L. Li, J. Huang, and X. Ji, "Lateral pressures on retaining wall of composite foundation in clayey soils," *Chinese Journal of Geotechnical Engineering*, vol. 41, no. 1, pp. 89–92, 2019.
- [33] M. Li, Y. Qian, Y. Guo, Y. Wei, S. Zhao, and X. Cui, "Design of lateral soil pressure model test scheme for adjacent composite foundation," *Mechanics in Engineering*, vol. 41, no. 2, pp. 157–163, 2019.
- [34] L. Li, H. Zhang, B. Xu, and Y. Wang, "Optimization of excavation supporting structure considering lateral reinforcement effect of CFG composite foundation on soils," *Chinese Journal of Geotechnical Engineering*, vol. 34, pp. 500–506, 2012.
- [35] L. Li, J. Huang, and B. Han, "Centrifugal investigation of excavation adjacent to existing composite foundation," *Journal of Performance of Constructed Facilities*, vol. 32, no. 4, Article ID 04018044, 2018.
- [36] Q. X. Ji and X. S. Ge, "The research on the influence of the forms of foundation on the behavior of adjacent excavation based on building materials," *Advanced Materials Research*, vol. 788, pp. 606–610, 2013.
- [37] Y. Wei, *Research on evolutionary mechanisms and calculation method of earth pressure against rigid retaining walls close to rigid composite foundation*, Ph.D dissertation, Zhengzhou University, Zhengzhou, China, 2018.
- [38] G.-H. Wang and Y.-Y. Yang, "Effect of cantilever soldier pile foundation excavation closing to an existing composite foundation," *Journal of Central South University*, vol. 20, no. 5, pp. 1384–1396, 2013.
- [39] Q. Fu and L. Li, "Vertical load transfer behavior of composite foundation and its responses to adjacent excavation: centrifuge model test," *Geotechnical Testing Journal*, vol. 44, no. 1, Article ID 20180237, 2021.
- [40] M. Li, Y. Qian, Y. Guo, and Y. Wei, "Study on Influence of retaining wall rotation on load distribution of rigid pile composite foundation," *Journal of Shenyang Jianzhu University (Natural Science)*, vol. 35, no. 4, pp. 655–662, 2019.
- [41] L. F. Miao, A. T. C. Goh, K. S. Wong, and C. I. Teh, "Three-dimensional finite element analyses of passive pile behaviour," *International Journal for Numerical and Analytical Methods in Geomechanics*, vol. 30, no. 7, pp. 599–613, 2006.
- [42] M. Yang, X. Dai, M. Zhang, and H. Luo, "Experimental study on earth pressure of cohesionless soil with limited width behind retaining wall," *Chinese Journal of Geotechnical Engineering*, vol. 38, no. 1, pp. 131–137, 2016.
- [43] K. Horikoshi and M. F. Randolph, "On the definition of raft-soil stiffness ratio for rectangular rafts," *Géotechnique*, vol. 47, no. 5, pp. 1055–1061, 1997.
- [44] V. Fioravante, "On the shaft friction modelling of non-displacement piles in sand," *Soils and Foundations*, vol. 42, no. 2, pp. 23–33, 2002.
- [45] R. Nishanthan, D. S. Liyanapathirana, and C. J. Leo, "Shielding effect in pile groups adjacent to deep unbraced and braced excavations," *International Journal of Geotechnical Engineering*, vol. 11, no. 2, pp. 162–174, 2017.
- [46] C. H. Juang, W. Gong, J. R. Martin, and Q. Chen, "Model selection in geological and geotechnical engineering in the face of uncertainty—does a complex model always outperform a simple model?" *Engineering Geology*, vol. 242, pp. 184–196, 2018.
- [47] M. N. Hussien, E. H. Ramadan, M. H. Hussein, A. A. A. Senoon, and M. Karray, "Load sharing ratio of pile-raft system in loose sand: an experimental investigation," *International Journal of Geotechnical Engineering*, vol. 11, no. 5, pp. 524–529, 2017.
- [48] Q. N. Pham, S. Ohtsuka, K. Isobe, and Y. Fukumoto, "Group effect on ultimate lateral resistance of piles against uniform ground movement," *Soils and Foundations*, vol. 59, no. 1, pp. 27–40, 2019.
- [49] Q.-Q. Zhang, S.-W. Liu, R.-F. Feng, J.-G. Qian, and C.-Y. Cui, "Finite element prediction on the response of non-uniformly arranged pile groups considering progressive failure of pile-soil system," *Frontiers of Structural and Civil Engineering*, vol. 14, no. 4, pp. 961–982, 2020.
- [50] M. Samanta and R. Bhowmik, "3D numerical analysis of piled raft foundation in stone column improved soft soil," *International Journal of Geotechnical Engineering*, vol. 13, no. 5, pp. 474–483, 2019.
- [51] M. A. Soomro, D. A. Mangnejo, R. Bhanbhro, N. A. Memon, and M. A. Memon, "3D finite element analysis of pile responses to adjacent excavation in soft clay: effects of different excavation depths systems relative to a floating pile,"

- Tunnelling and Underground Space Technology*, vol. 86, pp. 138–155, 2019.
- [52] S. Boussetta, M. Bouassida, and M. Zouabi, “Assessment of observed behavior of soil reinforced by rigid inclusions,” *Innovative Infrastructure Solutions*, vol. 1, no. 1, p. 27, 2016.
- [53] S. Boussetta, M. Bouassida, A. Dinh, J. Canou, and J. Dupla, “Physical modeling of load transfer in reinforced soil by rigid inclusions,” *International Journal of Geotechnical Engineering*, vol. 6, no. 3, pp. 331–342, 2012.
- [54] P. Bui, Q. Luo, L. Zhang, and M. Zhang, “Geotechnical centrifuge experiment model on analysis of pile-soil load share ratio on composite foundation of high strength concrete pile,” in *Proceedings of the International Conference on Transportation Engineering 2009 Presented at the Second International Conference on Transportation Engineering*, pp. 3465–3470, American Society of Civil Engineers, Southwest Jiaotong University, Chengdu, China, July 2009.
- [55] V. D. Tran, J.-J. Richard, and T. Hoang, “Soft soil improvement using rigid inclusions: toward an application for transport infrastructure construction in vietnam,” in *New Prospects in Geotechnical Engineering Aspects of Civil Infrastructures*, H. K. Vietnam, H. Youn, and M. Bouassida, Eds., Springer International Publishing, New York, NY, USA, pp. 89–99, 2019.
- [56] W. Liu, X. Yang, S. Zhang, X. Kong, and W. Chen, “Analysis of deformation characteristics of long-short pile composite foundation in salt lake area, Iran,” *Advances in Civil Engineering*, vol. 2019, Article ID 5976540, 15 pages, 2019.
- [57] Y. Lv, X. Ding, and D. Wang, “Effects of the tip location on single piles subjected to surcharge and axial loads,” *Science World Journal*, vol. 2013, Article ID 149706, 2013.
- [58] D. S. Liyanapathirana and R. Nishanthan, “Influence of deep excavation induced ground movements on adjacent piles,” *Tunnelling and Underground Space Technology*, vol. 52, pp. 168–181, 2016.
- [59] A. Saeedi Azizkandi, H. Rasouli, and M. H. Baziar, “Load sharing and carrying mechanism of piles in non-connected pile rafts using a numerical approach,” *International Journal of Civil Engineering*, vol. 17, no. 6, pp. 793–808, 2019.
- [60] Y. P. Dong, H. J. Burd, and G. T. Houlsby, “Finite element parametric study of the performance of a deep excavation,” *Soils and Foundations*, vol. 58, no. 3, pp. 729–743, 2018.
- [61] C. F. Leung, J. K. Lim, R. F. Shen, and Y. K. Chow, “Behavior of pile groups subject to excavation-induced soil movement,” *Journal of Geotechnical and Geoenvironmental Engineering*, vol. 129, no. 1, pp. 58–65, 2003.
- [62] L. Li and Q. Fu, “Lateral mechanical behavior of composite ground due to adjacent excavation: centrifuge model test,” *China Civil Engineering Journal*, vol. 50, no. 6, pp. 85–94, 2017.
- [63] F. Foroughi Boroujeni and R. Porhoseini, “Effect of execution process on pile group-excavation interaction,” *International Journal of Geotechnical Engineering*, pp. 1–9, 2020.
- [64] Y.-Y. Liang, N.-W. Liu, F. Yu, X.-N. Gong, and Y.-T. Chen, “Prediction of response of existing building piles to adjacent deep excavation in soft clay,” *Advances in Civil Engineering*, vol. 2019, Article ID 8914708, 11 pages, 2019.
- [65] R. Zhang, W. Zhang, and A. T. C. Goh, “Numerical investigation of pile responses caused by adjacent braced excavation in soft clays,” *International Journal of Geotechnical Engineering*, vol. 15, no. 7, pp. 783–797, 2018.
- [66] D. E. L. Ong, C. F. Leung, Y. K. Chow, and T. G. Ng, “Severe damage of a pile group due to slope failure,” *Journal of Geotechnical and Geoenvironmental Engineering*, vol. 141, no. 5, Article ID 04015014, 2015.
- [67] M. T. Suleiman, L. Ni, J. D. Helm, and A. Raich, “Soil-pile interaction for a small diameter pile embedded in granular soil subjected to passive loading,” *Journal of Geotechnical and Geoenvironmental Engineering*, vol. 140, no. 5, Article ID 04014002, 2014.
- [68] H. G. Poulos and L. T. Chen, “Pile response due to excavation-induced lateral soil movement,” *Journal of Geotechnical and Geoenvironmental Engineering*, vol. 123, no. 2, pp. 94–99, 1997.
- [69] M. A. Soomro, A. Saand, N. Mangi, D. A. Mangnejo, H. Karira, and K. Liu, “Numerical modelling of effects of different multipropelled excavation depths on adjacent single piles: comparison between floating and end-bearing pile responses,” *European Journal of Environmental and Civil Engineering*, pp. 1–31, 2019.
- [70] M. Shakeel and C. W. W. Ng, “Settlement and load transfer mechanism of a pile group adjacent to a deep excavation in soft clay,” *Computers and Geotechnics*, vol. 96, pp. 55–72, 2018.
- [71] R. Zhang, J. Zheng, and S. Yu, “Responses of piles subjected to excavation-induced vertical soil movement considering unloading effect and interfacial slip characteristics,” *Tunnelling and Underground Space Technology*, vol. 36, pp. 66–79, 2013.